Volume 1 | Number 1 | Jan 2013 | Pages 1–100

Dalton Transactions

An international journal of inorganic chemistry
www.rsc.org/dalton

ROYAL SOCIETY OF CHEMISTRY

This is an *Accepted Manuscript*, which has been through the Royal Society of Chemistry peer review process and has been accepted for publication.

Accepted Manuscripts are published online shortly after acceptance, before technical editing, formatting and proof reading. Using this free service, authors can make their results available to the community, in citable form, before we publish the edited article. We will replace this *Accepted Manuscript* with the edited and formatted *Advance Article* as soon as it is available.

You can find more information about *Accepted Manuscripts* in the **Information for Authors**.

Please note that technical editing may introduce minor changes to the text and/or graphics, which may alter content. The journal's standard **Terms & Conditions** and the **Ethical guidelines** still apply. In no event shall the Royal Society of Chemistry be held responsible for any errors or omissions in this *Accepted Manuscript* or any consequences arising from the use of any information it contains.

Journal Name

COMMUNICATION

Synthesis and catalytic application of PVP-coated Ru nanoparticles embedded in a porous metal–organic framework

Masaaki Sadakiyo,[a,b] Masaru Kon-no,[a] Katsutoshi Sato,[c,d] Katsutoshi Nagaoka,[b,d] Hidetaka Kasai,[b,e] Kenichi Kato,[b,e] and Miho Yamauchi*[a,b,f]

A hybrid catalyst consisting of polymer-coated Ru nanoparticles (Ru-PVP, PVP: poly(N-vinyl-2-pyrrolidone)) embedded in a porous metal–organic framework of ZIF-8 (Ru-PVP@ZIF-8) was synthesized by the crystallization of ZIF-8 in a methanol solution of Ru-PVP. Structural properties of Ru-PVP@ZIF-8 were examined by N_2 gas adsorption, infrared spectrum, and X-ray powder diffraction measurements. We successfully identified the most appropriate pretreatment condition for surface activation of the Ru nanoparticles in the catalyst. The pretreated Ru-PVP@ZIF-8 was applied for a CO oxidation reaction with H_2 gas feeds. Ru-PVP@ZIF-8 was found to exhibit higher catalytic activities and higher CO_2 selectivity than those observed on a carbon-supported Ru-PVP (Ru-PVP/C), implying that the pores of the ZIF-8 provide a more suitable environment for the reaction with O_2 and CO gases.

Ruthenium is one of the most important elements for catalytic reactions because of its wide applicability including preferential CO oxidation,[1-2] Fischer–Tropsch synthesis,[3-4] ammonia synthesis,[5-6] and decomposition.[7] Ru catalysts where nanoparticles (NPs) of Ru are dispersed on porous carbon or metal oxides are commonly studied for these reactions. Metal–organic frameworks (MOFs) have attracted much interest as a new class of porous solids showing various functionalities such as separation,[8] gas storage,[9-10] controlled delivery,[11] magnetism,[12] and conductive property.[13-15] Recently, designable architectures of MOFs have emerged as a new type of support material applicable to the heterogeneous catalysis because of their high surface area, porosity, and various chemical interactions with substrates.[16] Composites of metal NPs and MOF supports were prepared as catalysts by solid grinding,[17] impregnation,[18] gas-phase infiltration,[19] and encapsulation methods.[20] However, few examples of catalysis using the Ru-MOF composite[18,21] have been reported. Here, we perform a synthesis, characterization, and catalytic reaction of a composite of Ru NPs and MOF. We employ the third method using Ru NPs and $[Zn(mIM)_2]_n$ (ZIF-8, HmIM: 2-methylimidazole),[22] as reported by Huo and Hupp et al.,[20] to take advantage of the thermal and moisture stability of a framework.

Ru NPs coated with PVP (abbreviated to Ru-PVP, PVP = poly(N-vinyl-2-pyrrolidone)) were synthesized by heating a mixture of $RuCl_3 \cdot nH_2O$, PVP, and ethylene glycol at 190 °C. Ru-PVP was obtained by centrifugation of the mixture and was washed several times with a mixed solvent of water and acetone (details are shown in the Electronic Supplementary Information (ESI)). The catalyst of Ru-PVP embedded in ZIF-8 (Ru-PVP@ZIF-8) was prepared by mixing a methanol solution of $Zn(NO_3)_2 \cdot 6H_2O$ and HmIM with a methanol suspension of Ru-PVP.[20] After maintaining the catalyst at room temperature for 24 h, Ru-PVP@ZIF-8 was separated by centrifugation, washed by methanol, and dried under vacuum at room temperature (see the ESI). We also synthesized PVP-coated Ru NPs supported on carbnon (Ru-PVP/C) for comparison (see the ESI). The Ru-PVP@ZIF-8 and Ru-PVP/C were estimated, by using energy-dispersive X-ray (EDX) spectrometry, to be comprised of 5 wt% Ru element.
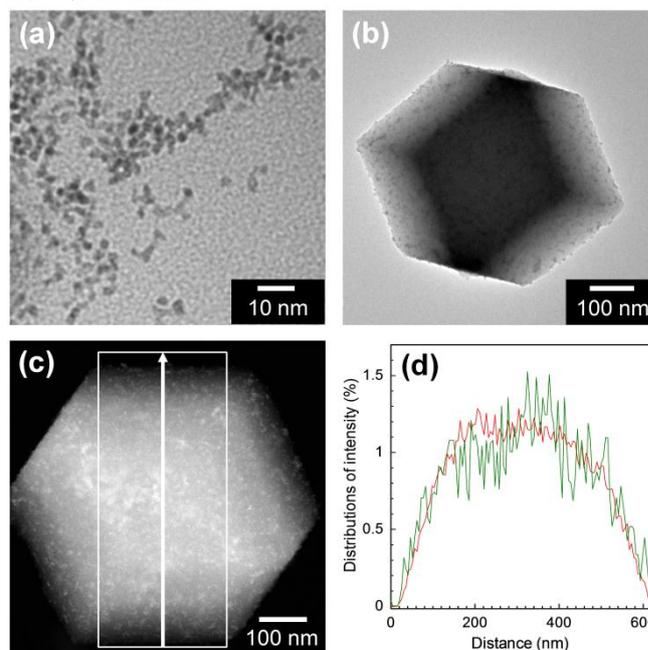
Fig. 1 TEM images of (a) **Ru-PVP** and (b) **Ru-PVP@ZIF-8**. (c) HAADF-STEM image of **Ru-PVP@ZIF-8** and (d) spatial

distributions of STEM-EDX signals of Zn-L (red) and Ru-L (green) integrated in the area surrounded by a white square along a white arrow shown in (c). The intensity at each position is normalized by total intensity in the square.

A transmission electron microscope (TEM) was used to observe the size of the Ru NPs in **Ru-PVP** and **Ru-PVP@ZIF-8**. After counting 200 particles on the TEM images (shown in Figure 1a), the mean diameter of Ru NPs in **Ru-PVP** was calculated to be 1.6 ± 0.4 nm. Figure 1b shows that Ru NPs seem to be located in a hexagonal-shaped ZIF-8 microcrystal.[20] To get clear evidence for the existence of Ru NPs embedded in **Ru-PVP@ZIF-8**, we also performed high-angle annular dark-field scanning TEM (HAADF-STEM) observation (Figures 1c and S2) and STEM-EDX analysis (Figure 1d). As shown in the figure 1c and S2, Ru NPs are uniformly dispersed in a ZIF-8 crystal even a part of Ru NPs are located on the surface of the crystal. Spatial distribution of Zn and Ru elements in **Ru-PVP@ZIF-8** was obtained by integration of Zn-L and Ru-L STEM-EDX as shown in Figure 1d. We can recognize that the Ru distribution indicates the same tendency of the distribution of Zn ions that are located inside **Ru-PVP@ZIF-8**. This clearly suggests that the Ru NPs are uniformly dispersed in a ZIF-8 crystal and a large percentage of Ru atoms are included in the ZIF-8 medium. The mean diameter of Ru NPs in **Ru-PVP@ZIF-8** was found to be 1.7 ± 0.4 nm, which is nearly equal to the mean diameter of **Ru-PVP**. These results indicate that the **Ru-PVP** is successfully embedded in the ZIF-8. In addition, we found that Ru NPs in **Ru-PVP/C** also have a similar mean diameter of 1.5 ± 0.3 nm (Figure S1).

X-ray powder diffraction (XRPD) measurements were taken to check the structure of Ru NPs and ZIF-8 crystals. Figures S3 and S4 show XRPD patterns of **Ru-PVP** and **Ru-PVP@ZIF-8** (see the ESI). The **Ru-PVP** showed very broad diffraction peaks due to the small diameter of the particles. The **Ru-PVP** peak pattern was attributable to hcp structure, which reveals that metallic Ru NPs are formed. On the other hand, **Ru-PVP@ZIF-8** showed very sharp diffraction peaks that are characteristic of the ZIF-8 crystals (Figure S4). It was also apparent that peaks derived from Ru NP were difficult to recognize in the XRPD patterns of **Ru-PVP@ZIF-8**, while the existence of Ru nanoparticles was confirmed in the TEM observation.

We measured N_2 gas adsorption/desorption isotherms at 77 K (Figure S5) to investigate the porosity and guest accessibility of the ZIF-8 framework around Ru NPs in **Ru-PVP@ZIF-8**. N_2 gas was highly adsorbed at low pressure in **Ru-PVP@ZIF-8**, which is indicative of a type I isotherm. This indicates that the microporous framework is formed around Ru NPs and the gas substrate is diffusive in **Ru-PVP@ZIF-8**. From an analysis of the absorption isotherm, the BET surface area of **Ru-PVP@ZIF-8** was estimated to be 1460 m^2 g^{-1}, which is somewhat smaller than the surface area of the blank ZIF-8 (1664 m^2 g^{-1}, BET). The decrease of surface area is due to the difference in the ZIF-8 content (ZIF-8 90 wt%, Ru 5 wt%, and PVP 5 wt%) in **Ru-PVP@ZIF-8**, which was evident from the elemental analysis and, therefore, the ZIF-8 framework in **Ru-PVP@ZIF-8** has empty pores similar to the blank one.

In general, certain appropriate pretreatment of a metal catalyst is required to recover its metallic surface before application to catalytic reactions. First, we performed thermogravimetric analysis (TGA) with a H_2 gas feed. As shown in Figure S6, a large weight loss around 300 °C was observed in **Ru-PVP@ZIF-8**, which is attributable to the decomposition of PVP. Analogously to the blank ZIF-8, **Ru-PVP@ZIF-8** was stable below 500 °C. We also

measured the infrared (IR) spectra of the samples treated at various temperatures with a H_2 gas atmosphere (Figure S7). The peak of the stretching mode of the carbonyl group on PVP at 1680 cm^{-1} disappears on **Ru-PVP@ZIF-8** after being treated at temperatures exceeding 400 °C (see Figure S7). This clearly indicates that the PVP in the **Ru-PVP@ZIF-8** can be removed by heat treatment at temperatures exceeding 400 °C. The other peaks derived from the ZIF-8 framework (from 650 to 1600 cm^{-1}) did not show significant changes by heat treatment below 500 °C, suggesting that the ZIF-8 framework does not decompose when temperature is less than 500 °C. The XRPD pattern of **Ru-PVP@ZIF-8** was almost unchanged after the heat treatment at 500 °C, which also supports that the crystal structure of ZIF-8 framework remains after this heat treatment (Figure S8).
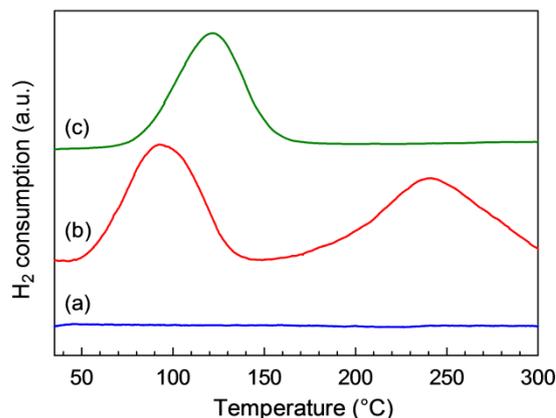
Fig. 2 TPR profiles of (a) ZIF-8, (b) **Ru-PVP@ZIF-8**, and (c) **Ru-PVP@ZIF-8** treated with a H_2 gas feed at 500 °C.

We performed temperature-programmed reduction (TPR) measurements using 5% H_2/Ar mixed gas to evaluate favourable pretreatment conditions for catalytic application of **Ru-PVP@ZIF-8**. Figure 2 shows the TPR profiles of ZIF-8, **Ru-PVP@ZIF-8**, and **Ru-PVP@ZIF-8** treated with a H_2 gas feed at 500 °C (described as **Ru@ZIF-8** hereafter). One peak is observed around 120 °C in the profile for **Ru@ZIF-8** and two peaks around 100 and 240 °C for **Ru-PVP@ZIF-8**. Because the blank ZIF-8 does not show any reduction peaks, peaks observed for **Ru@ZIF-8** and **Ru-PVP@ZIF-8** are due to H_2 consumption by the included **Ru-PVP**. Considering that the **Ru@ZIF-8** does not show any peaks above 200 °C, the peak observed around 240 °C on **Ru-PVP@ZIF-8** is due to the reductive decomposition of PVP and the first peak around 100 °C is due to the reduction of the surface of Ru NPs. These results clearly suggest that the surface of Ru NPs in the ZIF-8 can be activated by thermal treatment above 150 °C with a 5% H_2/Ar mixed gas feed. It should be noted that this thermal treatment is also effective for activation of **Ru-PVP/C**, as illustrated in a TPR chart (Figure S9).
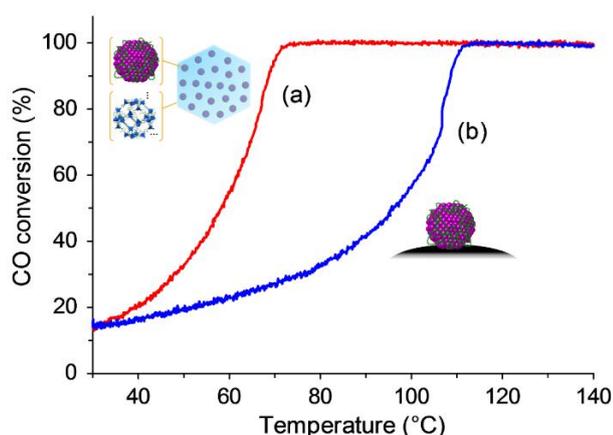
Fig. 3 CO conversions on (a) **Ru-PVP@ZIF-8** and (b) **Ru-PVP/C**. Before the catalytic reaction, samples were pretreated at 160 °C for 30 min with a 5% H_2/Ar mixed gas feed.

We examined catalytic activities of **Ru-PVP@ZIF-8** and **Ru-PVP/C** for CO oxidation reaction in H_2 gas feeds[1,23] using a reaction gas mixture of 0.1% CO, 0.5% O_2, 49.2% H_2, and 50.2% Ar. Figure S10 shows the CO conversions observed on **Ru-PVP@ZIF-8** before and after the pretreatment at 160 °C and the pretreated one after being treated further at 300, 400 and 500 °C with a H_2 gas feed. Activity for the reaction was negligible when a catalyst was used without pretreatment. In contrast, the pretreated one had high catalytic activity, indicating that the Ru surface was successfully activated by the removal of adsorbed oxygen atoms by the pretreatment at 160 °C. Note that the blank ZIF-8 did not show catalytic activity for the reaction, indicating that the CO oxidation reaction is catalysed by the included Ru NPs and that the gaseous reactants are accessible to the surface of Ru NPs surrounded by the porous ZIF-8 and PVP. On the other hand, activities of the catalysts treated at 300, 400, and 500 °C with H_2 gas feeds were lower, especially at higher treatment temperatures. Considering the results of TGA, IR, and TPR experiments, we assume that surface poisoning of Ru in the catalyst was a result of adsorption of decomposed matters of PVP or the physical contact between Ru NPs and ZIF-8 surfaces at high temperature. This assumption was examined by performing CO-pulse adsorption measurements. The samples were treated in a manner analogous to the CO oxidation reaction (160 °C for 30 min with 5% H_2/Ar mixed gas feeds) just before measurements. CO chemisorption amounts, for various **Ru-PVP@ZIF-8** catalysts, were measured as 12.8 (only 160 °C treatment), 2.50 (further pretreatment at 300 °C with a H_2 gas feed), 0.69 (at 400 °C), and 0.02 (at 500 °C) cm^3 g(Ru)$^{-1}$, respectively (Table S1). These results suggest that decreases in catalytic activity are due to surface poisoning of Ru NPs. Because the sample without H_2/Ar mixed gas pretreatment at 160 °C did not show CO chemisorption, it can be concluded that the heat treatment around 160 °C with 5% H_2/Ar mixed gas feeds can activate **Ru-PVP@ZIF-8** catalysts without the surface poisoning of Ru NPs.

Figure 3 shows CO conversions on the **Ru-PVP@ZIF-8** and **Ru-PVP/C**. The CO conversions increased at higher temperatures and reached 100%, indicating that both catalysts have sufficient activity for the CO oxidation reaction. There is a significant difference between the catalytic activity of **Ru-PVP@ZIF-8** and **Ru-PVP/C**. The CO oxidation reaction on **Ru-PVP@ZIF-8** started at lower temperature (the temperature at 50% CO conversion (T_{50}) is determined to be 60 °C.) than

Ru-PVP/C (T_{50} = 97 °C). The difference was likely due to the difference in the supports. Interestingly, the **Ru-PVP@ZIF-8** showed higher catalytic activity than **Ru-PVP/C** while the CO chemisorption amount of **Ru-PVP@ZIF-8** (12.8 cm^3 g(Ru)$^{-1}$) was similar to that of **Ru-PVP/C** (13.0 cm^3 g(Ru)$^{-1}$) (Table S1). This indicates that the ZIF-8 is preferable as a support material for the CO oxidation reaction. Ratio of O_2 used for CO oxidation to total consumption of O_2, i.e., CO_2 selectivity, was calculated from the conversions of O_2 and CO gases (Figures S11 and S12).[23] At temperatures less than 70 °C, the CO_2 selectivity on **Ru-PVP@ZIF-8** was higher than that on **Ru-PVP/C**, indicating that the ZIF-8 framework is also preferable for the selective CO oxidation in this temperature region. This suggests that particular adsorptive interactions of CO and O_2 gases to ZIF-8 are deeply related to catalytic selectivity of **Ru-PVP@ZIF-8**.

In conclusion, we synthesized Ru NPs embedded in a porous metal–organic framework of ZIF-8 and measured high catalytic activity of **Ru-PVP@ZIF-8** for the CO oxidation reaction with H_2 gas feeds. The activation condition of the catalyst was optimized, whereby **Ru-PVP@ZIF-8** treated with 5% H_2/Ar mixed gas around 160 °C exhibited the best catalytic performance. The activity of **Ru-PVP@ZIF-8** catalyst was found to be lower at higher treatment temperatures because surface poisoning of Ru NPs occurred. Finally, it should be emphasized that the porous framework of ZIF-8 provides a more suitable environment for the CO oxidation on Ru NPs.

Acknowledgements

Notes and references

^{a} International Institute for Carbon-Neutral Energy Research (WPI-I2CNER), Kyushu University, 744 Moto-oka, Nishi-ku, Fukuoka 819-0395, Japan. E-mail: yamauchi@i2cner.kyushu-u.ac.jp; Fax: +81 92-802-6874; Tel: +81 92-802-6874

^{b} Core Research for Evolutional Science and Technology (CREST), Japan Science and Technology Agency (JST), 7 Goban-cho, Chiyoda-ku, Tokyo 102-0076, Japan

^{c} Elements Strategy Initiative for Catalysts and Batteries, Kyoto University, 1-30 Goryo-Ohara, Nishikyo-ku, Kyoto 615-8245, Japan

^{d} Department of Applied Chemistry, Faculty of Engineering, Oita University, 700 Dannoharu, Oita 870-1192, Japan

^{e} RIKEN SPring-8 Center, 1-1-1 Kouto, Sayo-cho, Sayo-gun, Hyogo 679-5148, Japan

^{f} Department of Chemistry, Faculty of Science, Kyushu University, Hakozaki 6-10-1, Higashi-ku, Fukuoka 812-8581, Japan

† Electronic Supplementary Information (ESI) available: Experimental details and supporting results. See DOI: 10.1039/c000000x/

1   S. Alayoglu, A. U. Nilekar, M. Mavrikakis, B. Eichhorn, *Nat. Mater.* **2008**, *7*, 333–338.
2   S. Y. Chin, O. S. Alexeev, M. D. Amirids, *Appl. Catal. A* **2005**, *286*, 157–166.
3   D. L. King, *J. Catal.* **1978**, *51*, 386–397.

4   E. Iglesia, S. L. Soled, R. A. Fiato, G. H. Via, *J. Catal.* **1993**, *143*, 345–368.

5   K. Aika, A. Ozaki, H. Hori, *J. Catal.* **1972**, *27*, 424–431.

6   M. Kitano, Y. Inoue, Y. Yamazaki, F. Hayashi, S. Kanbara, S. Matsuishi, T. Yokoyama, S.-W. Kim, M. Hara, H. Hosono, *Nat. Chem.* **2012**, *4*, 934–940.

7   T. V. Choudhary, C. Sivadinarayana, D. W. Goodman, *Catal. Lett.* **2001**, *3–4*, 197–201.

8   J. R. Li, J. Sculley, H. C. Zhou, *Chem. Rev.* **2011**, *112*, 869–932.

9   N. L. Rosi, J. Eckert, M. Eddaoudi, D. T. Vodak, J. Kim, M. O'Keeffe, O. M. Yaghi, *Science* **2003**, *300*, 1127–1129.

10 L. J. Murray, M. Dinca, J. R. Long, *Chem. Soc. Rev.* **2009**, *38*, 1294–1314.

11 P. Horcajada, T. Chalati, C. Serre, B. Gillet, C. Sebrie, T. Baati, J. F. Eubank, D. Heurtaux, P. Clayette, C. Kreuz, J.-S. Chang, Y. K. Hwang, V. Marsaud, P.-N. Bories, L. G. S. Cynober, G. Férey, P. Couvreur, R. Gref, *Nat. Mater.* **2010**, *9*, 172–178.

12 M. Kurmoo, *Chem. Soc. Rev.* **2009**, *38*, 1353-1379.

13 M. Sadakiyo, T. Yamada, H. Kitagawa, *J. Am. Chem. Soc.* **2009**, *131*, 9906–9907.

14 S. Bureekaew, S. Horike, M. Higuchi, M. Mizuno, T. Kawamura, D. Tanaka, N. Yanai, S. Kitagawa, *Nat. Mater.* **2009**, *8*, 831-836.

15 M. Sadakiyo, H. Kasai, K. Kato, M. Takata, M. Yamauchi, *J. Am. Chem. Soc.* **2014**, *136*, 1702–1705.

16 M. Meilikhov, K. Yusenko, D. Esken, S. Turner, G. V. Tendeloo, R. A. Fischer, *Eur. J. Inorg. Chem.* **2010**, 3701–3714.

17 H.-L. Jiang, B. Liu, T. Akita, M. Haruta, H. Sakurai, Q. Xu, *J. Am. Chem. Soc.* **2009**, *131*, 11302–11303.

18 X. Gu, Z.-H. Lu, H.-L. Jiang, T. Akita, Q. Xu, *J. Am. Chem. Soc.* **2011**, *133*, 11822–11825.

19 S. Hermes, M.-K. Schröter, R. Schmid, L. Khodeir, M. Muhler, A. Tissler, R. W. Fischer, R. A. Fischer, *Angew. Chem. Int. Ed.* **2005**, *44*, 6237–6241.

20 G. Lu, S. Li, Z. Guo, O. K. Farha, B. G. Hauser, X. Qi, Y. Wang, X. Wang, S. Han, X. Liu, J. S. DuChene, H. Zhang, Q. Zhang, X. Chen, J. Ma, S. C. J. Loo, W. D. Wei, Y. Yang, J. T. Hupp, F. Huo, *Nat. Chem.* **2012**, *4*, 310–316.

21 S. Turner, O. I. Lebedev, F. Schröder, D. Esken, R. A. Fischer, G. V. Tendeloo, *Chem. Mater.* **2008**, *20*, 5622–5627.

22 K. S. Park, Z. Ni, A. P. Cote, J. Y. Choi, R. Huang, F. J. Uribe-Romo, H. K. Chae, M. O'Keeffe, O. M. Yaghi, *PNAS* **2006**, *103*, 10186–10191.

23 P. V. Snytnikov, V. A. Sobyanin, V. D. Belyaev, P. G. Tsyrulnikov, N. B. Shitova, D. A. Shlyapin, *Appl. Catal. A* **2003**, *239*, 149–156.

Graphical abstract

A hybrid catalyst consisting of polymer-coated Ru nanoparticles (**Ru-PVP**, PVP: poly(N-vinyl-2-pyrrolidone)) embedded in a porous metal–organic framework of ZIF-8 (**Ru-PVP@ZIF-8**) was synthesized by the crystallization of ZIF-8 in a methanol solution of **Ru-PVP**. Structural properties of **Ru-PVP@ZIF-8** were examined by N_2 gas adsorption, infrared spectrum, and X-ray powder diffraction measurements. We successfully identified the most appropriate pretreatment condition for surface activation of the Ru nanoparticles in the catalyst. The pretreated **Ru-PVP@ZIF-8** was applied for a CO oxidation reaction with H_2 gas feeds. **Ru-PVP@ZIF-8** was found to exhibit higher catalytic activities and higher CO_2 selectivity than those observed on a carbon-supported **Ru-PVP** (**Ru-PVP/C**), implying that the pores of the ZIF-8 provide a more suitable environment for the reaction with O_2 and CO gases.